

# We are IntechOpen, the world's leading publisher of Open Access books Built by scientists, for scientists

6,900

Open access books available

186,000

International authors and editors

200M

Downloads

Our authors are among the

154

Countries delivered to

TOP 1%

most cited scientists

12.2%

Contributors from top 500 universities



WEB OF SCIENCE™

Selection of our books indexed in the Book Citation Index  
in Web of Science™ Core Collection (BKCI)

Interested in publishing with us?  
Contact [book.department@intechopen.com](mailto:book.department@intechopen.com)

Numbers displayed above are based on latest data collected.  
For more information visit [www.intechopen.com](http://www.intechopen.com)



## A Calibration-Free Evapotranspiration Mapping (CREMAP) Technique

József Szilágyi<sup>1,2</sup>, János Józsa<sup>1</sup> and Ákos Kovács<sup>1</sup>

<sup>1</sup>*Budapest University of Technology and Economics*

<sup>2</sup>*University of Nebraska-Lincoln*

<sup>1</sup>*Hungary*

<sup>2</sup>*USA*

### 1. Introduction

Obtaining spatially distributed accurate evapotranspiration (ET) estimates is crucial in most water balance calculations for the identification of mass and energy fluxes across the area of interest. While routine Bowen-ratio or eddy-covariance measurements of sensible and latent heat fluxes are typically representative of a horizontal scale of a few hundred meters (i.e., the so-called plot- or field-scale), many hydrologic models work at regional to continental to global scales. Rather than aggregating from the field scale, which may be difficult not only from a theoretical point of view but also from a practical one when long time-periods (years or decades) and large areas are considered, an ET-estimation technique that directly works at the regional scale, yet, at the same time, spatially distributed may be of high practical value.

An ET estimation method had been proposed by Bouchet (1963) almost half a century ago, now called the complementary relationship (CR) of evaporation which was subsequently formulated for practical regional-scale applications by Brutsaert & Stricker (1979), and Morton et al. (1985). The CR states that under constant available energy at the surface ( $Q_n$ ) actual ( $E$ ) and potential ( $E_p$ ) evapotranspiration rates are complementary, their sum yielding twice the wet-environment ( $E_w$ ) evapotranspiration rate, provided  $E_p$  is obtained by the Penman (1948) equation (Szilágyi & Józsa, 2009a) and  $E_w$  by the Priestley-Taylor equation (Priestley & Taylor, 1972). In other words

$$E = 2E_w - E_p \quad (1)$$

where

$$E_w = \alpha \frac{\Delta}{\Delta + \gamma} Q_n \quad (2)$$

with  $\Delta$  being the slope of the saturation vapor pressure curve at the temperature of the air,  $\gamma$  ( $\approx 0.67 \text{ hPa K}^{-1}$ ) the psychrometric constant, and  $\alpha$  the Priestley-Taylor coefficient with typical values within the interval of 1.2 - 1.3. Penman defined  $E_p$  (1948) as

$$E_p = \frac{\Delta}{\Delta + \gamma} Q_n + \frac{\gamma}{\Delta + \gamma} f(u)(e^* - e) \quad (3)$$

where  $e$  and  $e^*$  is the actual and saturation vapor pressure values (in hPa) at the temperature of the air, respectively, and the wind function,  $f(u)$  is defined as

$$f(u) = 0.26(1 + 0.54u_2) \quad (4)$$

with  $u_2$  ( $\text{m s}^{-1}$ ), the mean horizontal wind velocity, measured at 2-m height above the ground. With Eq. (4)  $E_p$  is given in  $\text{mm d}^{-1}$ , provided  $Q_n$  is also specified as water-depth equivalent in the same units.

While the Advection-Aridity (AA) model of Brutsaert & Stricker (1979) employs the above definitions for the different terms in Eq. (1), Morton et al. (1985) specify  $E_p$  and  $E_w$  differently in their WREVAP model, but in a way that Eq. (1) is still valid (Szilágyi & Józsa, 2008). They suggest Eq. (1) be employed for time-periods equal or longer than about a week (i.e., a minimum time-period of five days) for improved accuracy. This is so because the CR is based on an assumed dynamical equilibrium of the atmosphere and the underlying land surface, the latter influencing the humidity of the air through ET regulated by various feedbacks across the land-atmosphere interface. To attain such an equilibrium certainly takes some time in the wake of each weather front passing over the region.

In the past decade or so, Eq. (1) has been applied in several continental-scale studies ranging from specifying long-term mean ET across the conterminous US (e.g., Hobbins et al., 2001a,b) to identifying long-term trends in ET rates (Szilágyi, 2001), to investigating the global hydrologic cycle (Brutsaert & Parlange, 1998). While these studies yield regionally representative values of ET, none of them attempt to account for the spatial variability of ET within the region. Recently however Szilágyi & Józsa (2009b), employing the wet surface equation (Yeh & Brutsaert, 1971; Szilágyi & Józsa, 2009c), proposed such a disaggregation scheme utilizing Moderate Resolution Imaging Spectroradiometer (MODIS) data that have a nominal spatial resolution of about 1 km. Below a modified and simplified version of their ET mapping technique is explained with applications over two regions, Hungary in Central-Europe, and Nebraska in Central North America. To the best knowledge of the present authors no other calibration-free ET mapping technique exists that works at the watershed/regional scale and requires such a minimal and freely available input data as the current method to be discussed.

## 2. Description of the ET mapping approach

Spatial disaggregation of the regionally representative ET rates of Eq. (1), employing the AA (Brutsaert & Stricker, 1972) or WREVAP (Morton et al., 1985) models or the wet-surface equation (Yeh & Brutsaert, 1971; Szilágyi & Józsa, 2009c), is based on a linear transformation of the 8-day composited MODIS daytime surface temperature ( $T_s$ ) values into actual ET rates (Szilágyi & Józsa, 2009b). Compositing is used for eliminating cloud effects by retaining the warmest pixel value in each 8-day period. See the MODIS website ([modis.gsfc.nasa.gov](http://modis.gsfc.nasa.gov)) for more details of data collection and characteristics. The transformation requires the specification of two anchor points in the  $T_s$  - ET plane (Fig. 1). The first anchor point is defined by the spatially averaged daytime surface temperature,  $\langle T_s \rangle$ , and the corresponding regionally representative ET rate,  $E$ , from Eq. (1). The second anchor point results from a spatial averaging of the coldest pixel values,  $\langle T_{sw} \rangle$ , within the

region and  $E_w$  of Eq. (2) out of consideration that the coldest pixels are the wettest evaporating at the wet environment evapotranspiration rate,  $E_w$ . The two points define the linear transformation of the  $T_s$  pixel values into ET rates for each 8-day period, or, as was done by Szilágyi & Józsa (2009b) and repeated here, for each month by employing monthly means. The resulting line is extended to the right, since in about half of the pixels ET is less than the regional mean,  $E$ . A monthly time-step is ideal since most of the watershed- or large-scale hydrologic models work at this time-resolution, plus a monthly averaging further reduces any lingering cloud effect in the 8-day composited  $T_s$  values.

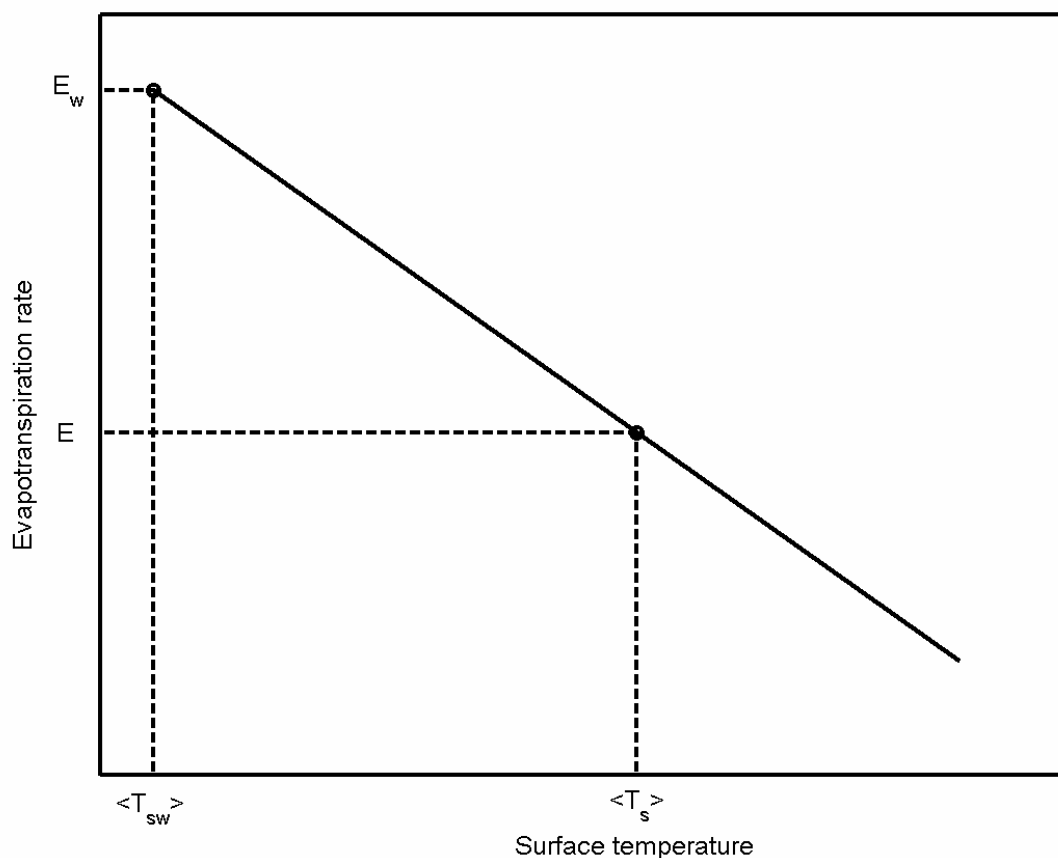


Fig. 1. Schematic representation of the linear transformation of the MODIS daytime surface temperature values into ET rates.

The linear transformation of Szilágyi & Józsa (2009b) can be derived through a generalization of the main idea that is behind the popular plot-scale ET-estimation models of SEBAL (Bastiaanssen et al., 1998) and METRIC (Allen et al., 2007). Namely, the vertical gradient of the air temperature near the surface can be assumed to be linearly dependent of the surface temperature (Bastiaanssen et al., 1998; Allen et al., 2007), thus the sensible heat ( $H$ ) transfer across the land-atmosphere interface, provided changes in the aerodynamic resistance ( $r_a$ ) among MODIS pixels are moderate, can also be taken a linear function of  $T_s$ . This can be so because under neutral atmospheric conditions (attained for time-steps a day or longer)  $r_a$  depends linearly on the logarithm of the momentum roughness height,  $z_{0m}$  (Allen et al., 2007), thus any change in  $z_{0m}$  between pixels becomes significantly dampened in the  $r_a$  value due to the logarithm. Consequently, the latent heat (LE) transfer itself becomes a linear function of  $T_s$  under a spatially constant  $Q_n$  term required by the CR, since

the soil heat flux is generally negligible for intervals longer than a day, therefore  $Q_n = H + LE$ , from which  $LE = mT_s + c$  follows,  $m$  and  $c$  being constants for the computational time step, i.e., a month here.

While a spatially constant  $Q_n$  term may, at first, seem an overly stringent requirement in practical applications due to spatial changes in vegetation cover as well as slope and aspect of the land surface,  $Q_n$  will change only negligibly in space provided the surface albedo also changes negligibly among the pixels over a flat or rolling terrain. The spatially constant  $Q_n$  (and to a lesser extent  $z_{0m}$ ) requirement thus limits the spatial resolution the current method can be applied at, since by decreasing the pixel size, heterogeneity among the cells surely increases. Below we show that at least for the study regions, the MODIS pixel size of about 1 km ensures a largely constant  $Q_n$  value among the pixels due to only small observed spatial changes in the mean monthly surface albedo value among the MODIS cells.

### 3. Application of the CREMAP ET mapping method

8-day composited MODIS daytime surface temperature data were collected for Hungary and Nebraska over the 2000 – 2008 and 2000 – 2009 periods, respectively. The 8-day composited pixel values were averaged for each month to obtain one surface temperature per pixel per month.

#### 3.1 Hungary

From the Hungarian Meteorological Service (HMS) 0.1-degree gridded mean monthly air temperature and specific humidity data were collected for the same period as well as sunshine duration values from 15 stations spread across the country which subsequently were interpolated to the same 0.1-degree grid. With these data, the linear transformation of mean monthly  $T_s$  values into monthly ET rates can be performed on a (MODIS) pixel-by-pixel basis. For validation purposes (a) 0.1-degree gridded precipitation ( $P$ ) data from HMS; (b) stream discharge ( $R$ ) values from the Water Resources Research Center (VITUKI), the University of West Hungary (NYME) and the Regional Water Authorities (RWA) for selected watersheds (Fig. 2); (c) eddy-covariance (EC) measurements of latent heat fluxes from HMS and the CarboEurope web-site ([www.carboeurope.org](http://www.carboeurope.org)) (Fig. 2); (d) lake evaporation measurements/estimates for Hungary's large shallow lakes (Balaton, Fertő, Velencei) from VITUKI and RWA were also collected.

The country due to its relatively small size was considered as one region which means that the linear transformation is valid for the whole country in the absence of elevation changes. However, with elevation, surface temperatures are expected to decrease independent of whether a pixel is wet or not. Therefore, the country was subdivided into three elevation zones: below 200 m, between 200 and 500 m, and above 500 m (Fig. 3). The anchor points of the linear transformation were calculated separately for the three zones each month by (a) calculating the spatial average of the MODIS-pixel surface temperatures within each zone and the corresponding regional evaporation rate,  $E$ , with the help of the WREVP program for which the input variables were the spatially averaged values of the 0.1-degree gridded air temperature, specific humidity and sunshine duration values within the zone; (b) calculating the wet-environment evaporation rate,  $E_w$ , within the zone by Eq. (2) (with  $\alpha = 1.26$ ) via the WREVP-estimated  $Q_n$  value plus taking the mean of the coldest 30-50 (30 in the highest region) MODIS pixels from the middle part (i.e., 300-400 m and 550-650 m, for the latter it was considered that the area vanishes fast with elevation) of the elevation zone.

For the lowest zone no such middle part was defined due to the small change in elevation. As Szilágyi & Józsa (2009b) demonstrated, the method is not sensitive to the exact number of cold pixels employed. Note that only the zone-averaged values of the 0.1-degree gridded meteorological data are needed for defining the anchor points, thus no matching of the MODIS and the 0.1-degree grid is required.

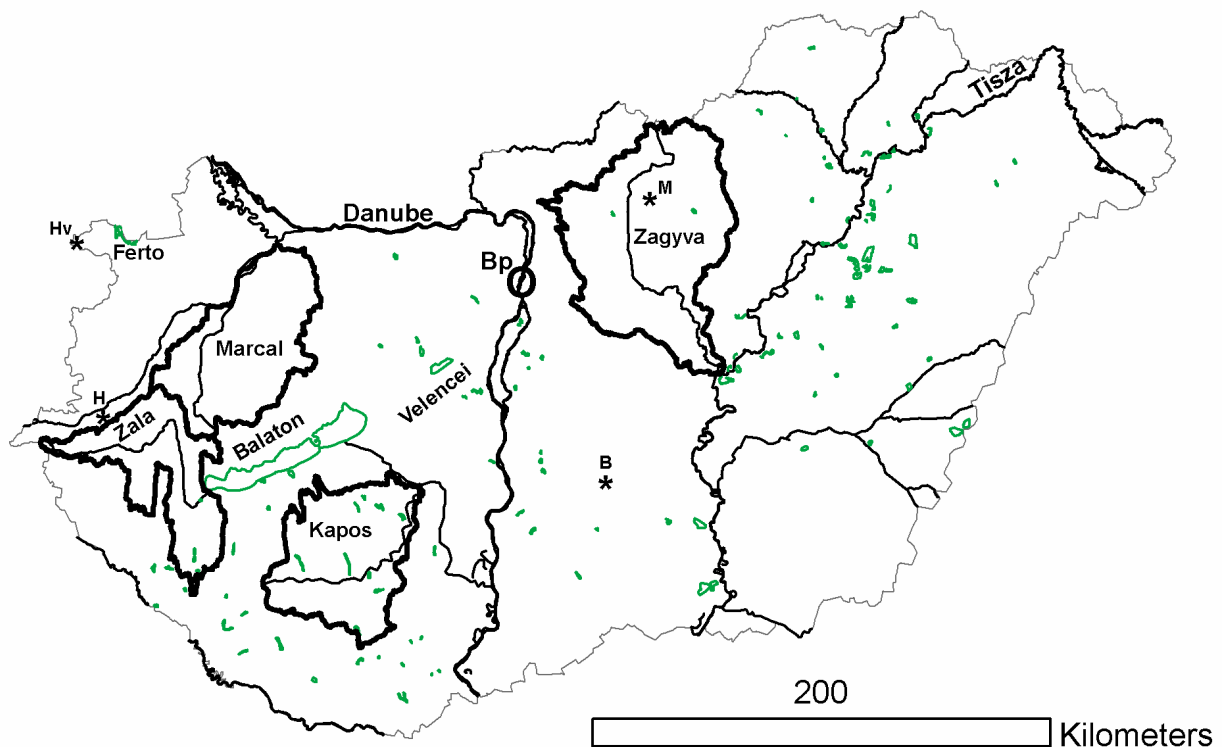


Fig. 2. Location of the watersheds [Kapos, Marcal, Zala, Zagyva and Hidegvizvolgy (Hv)] and eddy-covariance towers [Bugac (B), Matra (M), and Hegyhatsal (H)] used for validating the model estimates. The largest natural shallow lakes (denoted by green polygons, e.g., Balaton, Lakes Ferto and Velencei) of Hungary and the capital, Budapest (Bp) are also identified.

For avoiding possible sharp changes in the resulting pixel ET rates between the zones, the transformation equation was allowed to change linearly with pixel-elevation ( $z$ ) between the limiting equations of the lower ( $l$ ) and upper ( $u$ ) zones. Mathematically,

$$ET(z) = \frac{(z_u - z)[m_l T_s(z) + c_l] + (z - z_l)[m_u T_s(z) + c_u]}{z_u - z_l} \quad (5)$$

where  $m$  and  $c$  are the parameters of the linear transformations by zone, obtained with the help of the anchor points. Here the reference elevations ( $z_u$  or  $z_l$ ) are taken at 100, 350, and 600 meters.

Fig. 4 displays the linear transformations by months for the lowest zone (i.e., under 200 m). The line sections are bounded by the anchor points illustrated in Fig. 1 but during the calculations they are allowed to extend downward to accommodate for pixels warmer than the zonal-mean. Occasionally the transformation may yield negative pixel-ET values for very warm pixels which then were replaced by zeros. The lines, however, are bounded from above, i.e., in the few occasions (about half the number of the coldest points considered) when the pixel temperature is lower than  $\langle T_{ws} \rangle$ , the corresponding ET value assigned is still

$E_w$ , since at the 1-km scale this is the highest rate of ET achievable from energy considerations [i.e., the 1-km is the smallest scale for the validity of Eq. (2)].

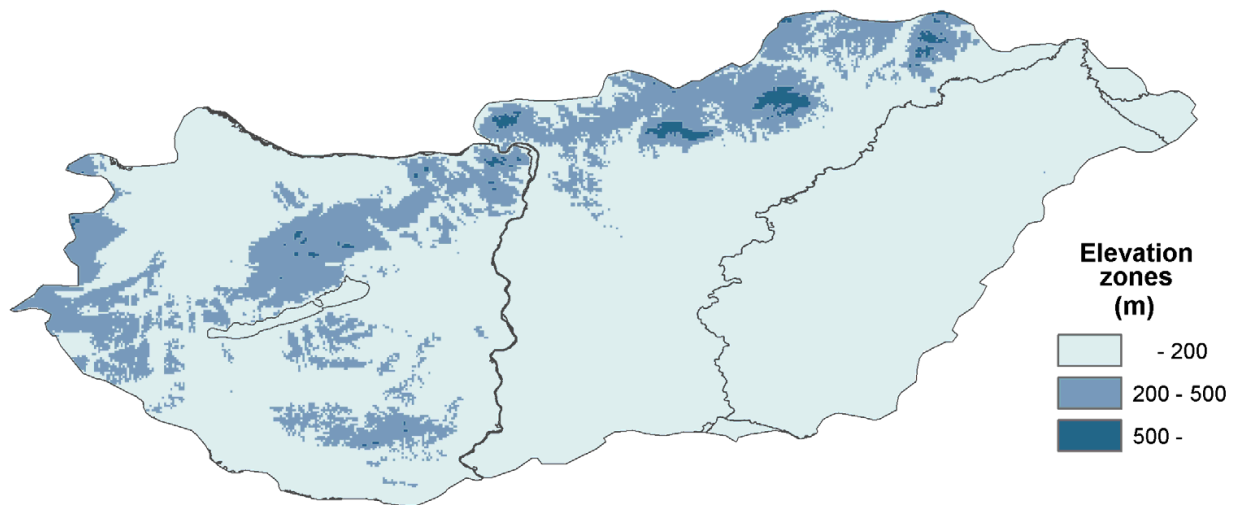


Fig. 3. The extent of the three elevation zones employed.

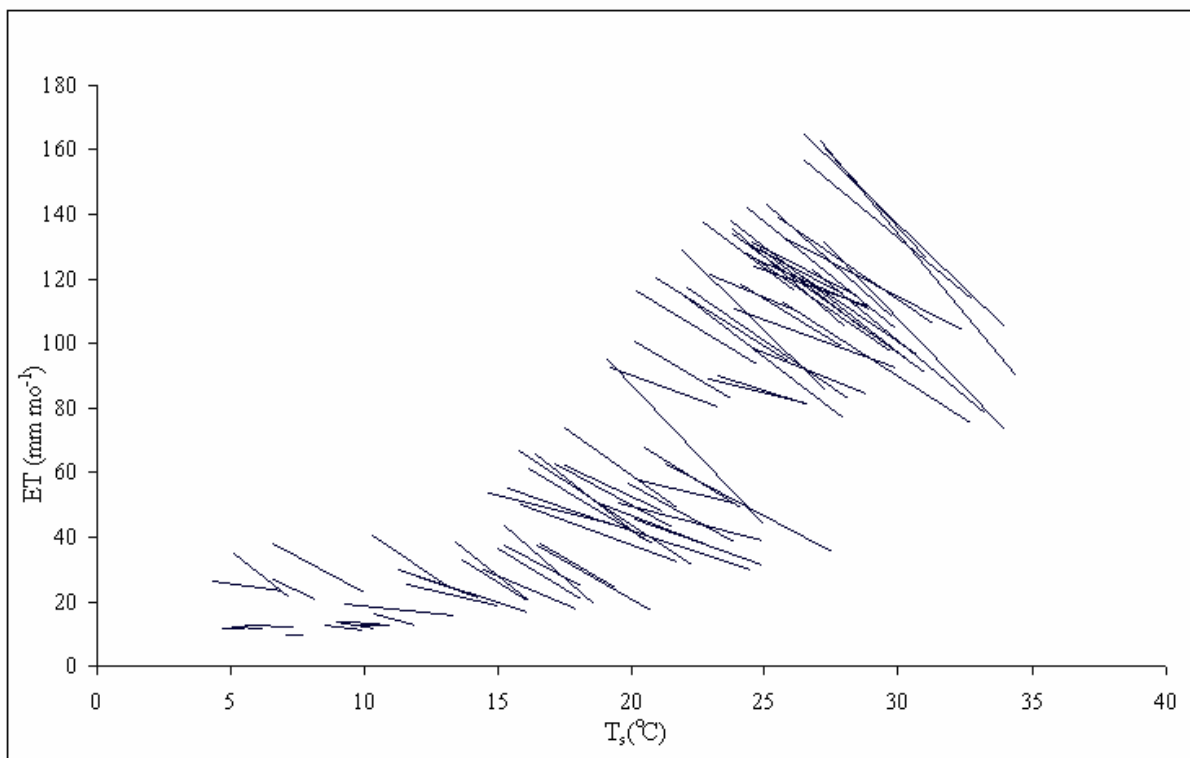


Fig. 4. Linear transformations for the lowest elevation zone in Hungary by month. Each line ends in the anchor points illustrated in Fig. 1. During the transformations the lines are extended downward to accommodate for pixels warmer than the zonal-mean.

The transformations were not performed for the winter months (December, January, and February) because then the ground may have patchy snow cover which violates the constant  $Q_n$  assumption since the albedo of snow is markedly different from that of the land. This is not a serious restriction on the general applicability of the model since in temperate climates ET is very limited in the winter months (with temperatures around 0 °C) anyway.

In the warm months the distribution of the albedo values among the MODIS cells is very narrow, with a standard deviation of about 1.6% and mean of 15%. This corroborates the working hypothesis that  $Q_n$  can be considered quasi-constant among the MODIS pixels. The only exception are the cells with open water. Open water surfaces have an albedo of around 5%, therefore the transformation-equation derived ET estimates are overwritten for such cells by the estimates of the lake evaporation module of WREVAP.

Table 1 displays the main characteristics of the ET validation sites and watersheds. Selection of the watersheds was limited mostly by data availability for the 2000-2008 period. Since the precipitation data (needed for back-calculating ET over the watershed as  $P - R$ ) provided by HMS is restricted to Hungary, only those watersheds could be considered that are fully within the country's boundary.

Location	Land cover	Coordinates (°) [lat (N), long]	Elevation (m a.s.l.)	Area (km <sup>2</sup> )
Hungary				
CarboEurope, Bugac (4-m tall EC tower)	Grassland	46.69, 19.6E	113	0.16
CarboEurope, Matra (3-m tall EC tower)	Vineyards/Orchards	47.85, 19.73E	300	0.09
Hegyhatsal (EC instr. at 82 m above ground)	Forest and cropland	46.95, 16.65E	248	67
Hidegvizvolgy catchm.	Forest	-	284 (mean)	6
Kapos catchment	Forest and cropland	-	184 (mean)	3210
Marcal catchment	Forest and cropland	-	185 (mean)	3042
Zagyva catchment	Forest and cropland	-	211 (mean)	4207
Zala catchment	Forest and cropland	-	195 (mean)	1528
Nebraska				
Sandhills, station #1 (2.68-m tall BR tower)	Sub-irrigated meadow	42.07, 101.47W	1087	0.07
station #2 (2.61-m tall BR tower)	Dry meadow	42.07, 101.44W	1081	0.07
station #3 (2.68-m tall BR tower)	Dunal upland grass	42.07, 101.37W	1086	0.07
Gothenburg (EC instr. at 7.8 m above canopy)	Riparian forest	40.92, 100.18W	783	0.61
Odessa (EC instrum. at 7.8 m above canopy)	Riparian forest	40.67, 99.22W	694	0.61
Mead, station #1 (4.5-m tall BR tower)	Irrigated maize	41.16, 96.47W	369	Varies < 0.2
station #2 (4.5-m tall BR tower)	Irrigated maize/soybean	41.16, 96.47W	369	Varies < 0.2
station #3 (4.5-m tall BR tower)	Non-irrigated maize/soybean	41.16, 96.47W	369	Varies < 0.2

Table 1. Validation sites and watersheds. EC: eddy covariance; BR: Bowen-ratio station. For the EC, BR sites, area means the estimated (100 times the height of the instrument above ground/canopy) footprint size.

### 3.2 Nebraska, USA

Mean annual precipitation, mean monthly maximum/minimum air and dew-point temperature values came from the PRISM database ([www.prism.oregonstate.edu](http://www.prism.oregonstate.edu)) at 2.5-min resolution. Mean monthly incident global radiation data at half-degree resolution were downloaded from the GCIP/SRB site ([www.atmos.umd.edu/~srb/gcip/cgi-bin/historic.cgi](http://www.atmos.umd.edu/~srb/gcip/cgi-bin/historic.cgi)). Due to its large size the state was subdivided into eight regions (Fig. 5) and the transformation equations calculated separately for each region, employing the coldest  $T_s$  value every month in each region and  $\alpha = 1.2$  in Eq. (2). For a smooth ET surface, the parameters of the transformation equations were linearly interpolated among all the cells.

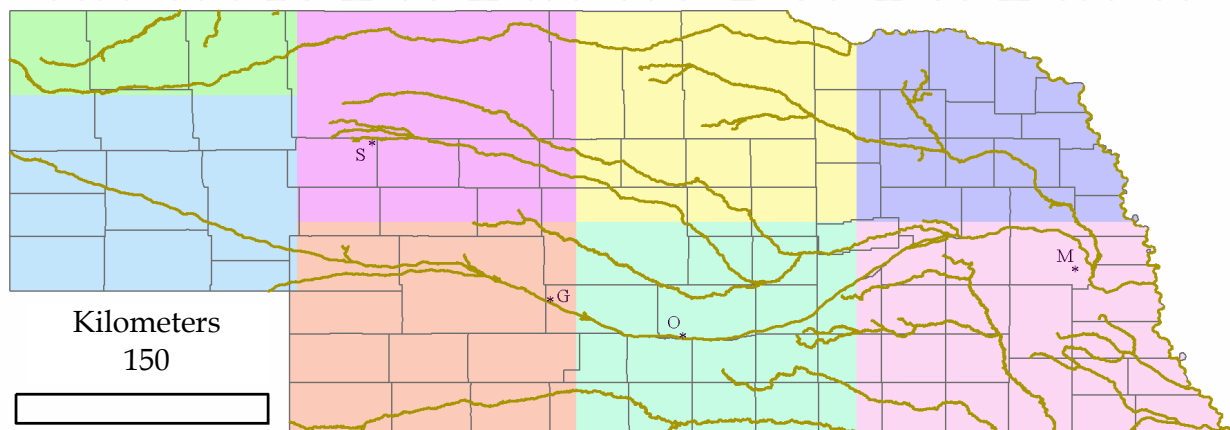


Fig. 5. Location of the validation sites (S: Sandhills; G: Gothenburg; O: Odessa; M: Mead) and the distribution of the eight regions.

As for Hungary, the transformations were performed only from March till November, each year. Due to the large size of the state, as well as the simultaneous presence of deep reservoirs and many small shallow lakes, CREMAP evaporation values were not corrected for open water surfaces. In a planned future online publication of the monthly maps, WREVAP-estimates of lake evaporation will be listed with the maps for each region: one estimate for a shallow, and a separate one for a deep open water body. See Table 1 for the characteristics of the validation sites.

## 4. Results and discussions

### 4.1 Hungary

Fig. 6 displays the spatial distribution of the ET rates as period-averaged (2000-2008) annual values. This is possible because we postulated that ET in the three winter months (with mean air temperatures around the freezing point) is negligible.

The driest continuous region is the sandy inter-fluvial plateau in south-central Hungary, the karstic-plateau just north of Lake Balaton, the urban conglomerate of Budapest and the southern side of the Matra mountain north-east of Budapest. The wettest regions are the mountains with good forest cover and ample precipitation in the north-eastern part of the country, the gallery-forests along the main rivers (the largest is Gemenc, a natural protection area along the Danube in the south-central part), the wetlands (Kis-Balaton, immediately south-west of Lake Balaton, as well as areas around Lake Fertő in north-western Hungary), and the forests in the south-western part of the country where annual precipitation is most

abundant, in excess of 800 mm. The evaporation rates of the largest water bodies (about 890 mm) were calculated by the WREVAP program with the winter months included since lake evaporation -- provided the lakes do not freeze up -- is typically not negligible even in cold temperatures. WREVAP has been shown to yield accurate estimates of lake evaporation. These evaporation rates are typically larger than the  $T_s$ -obtained values by about 10%, caused mainly by the difference in the albedo values of the two surfaces. For the calculations the otherwise hard-to-locate WREVAP documentation with the original FORTRAN source code of Morton et al. (1985) can be downloaded from the following web-site: <http://snr.unl.edu/szilagyi/szilagyi.htm>.

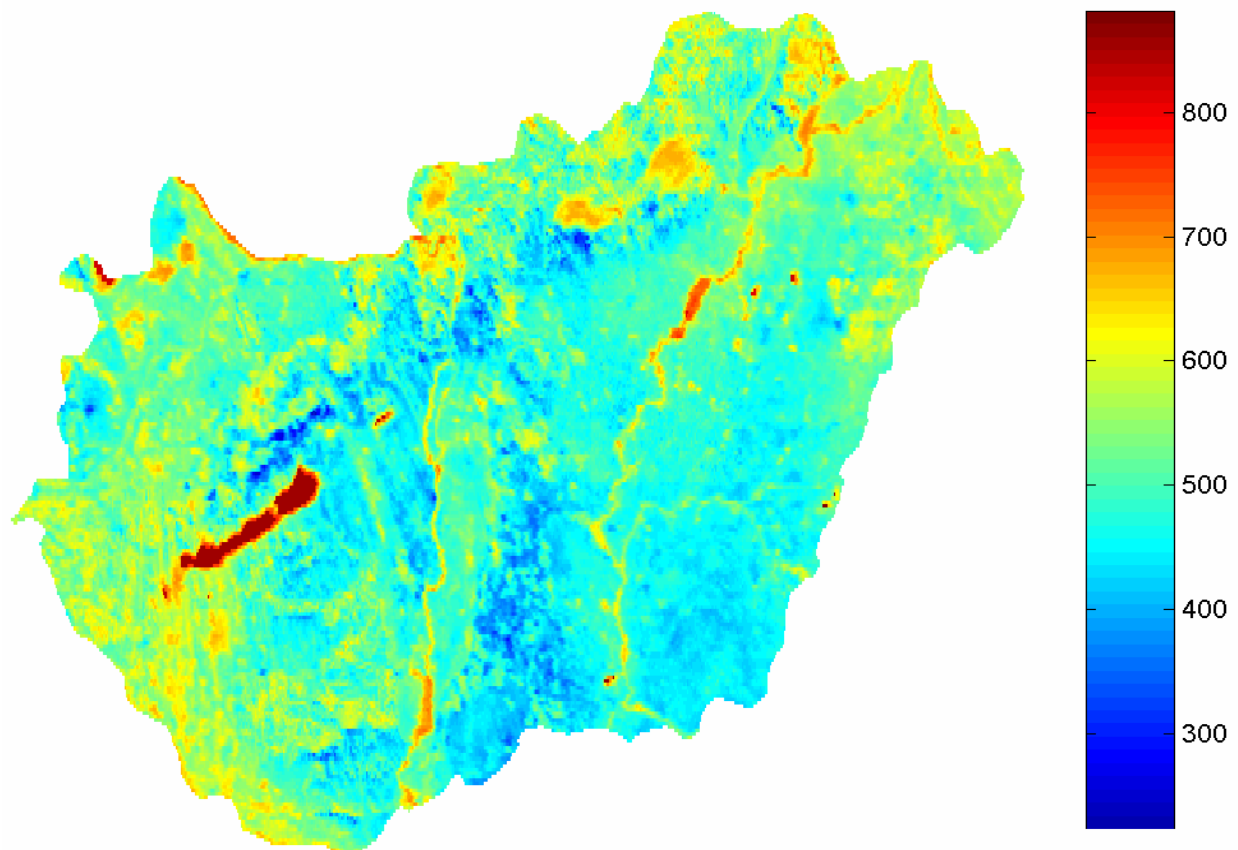


Fig. 6. Period-averaged (2000-2008) mean annual ET rates (mm) in Hungary.  $\langle ET \rangle = 510$  mm yr<sup>-1</sup>.

Validation of the results were performed with the help of three eddy-covariance sites and five watersheds (Fig. 2 and Tables 1 & 2). While continuous data from the two CarboEurope sites (Nagy et al., 2007; Pinter et al., 2008) were available for each month of our study period, from the third site, Hegyhatsal (Barcza et al., 2009), continuous measurements were available only for selected months. Here the CREMAP ET values (averaged over  $8 \times 8 = 64$  MODIS pixels around the tower) yield an unbiased estimates of the observed ET rates (Fig. 7), provided the Hegyhatsal measurements are multiplied by 1.78. This is necessary because the uncorrected eddy-covariance measurements represent a 44% systematic underestimation in comparison with energy balance closure. The  $Q_n$  values were obtained from two independent sources (a) locally measured data, and; (b) WREVAP-model

estimates based on 0.1-degree gridded sunshine duration measurements. The two  $Q_n$  means are within 5% reinforcing the accuracy of the net radiation measurements at Hegyhatsal and the systematic underestimation of the EC instruments.

Location	Monthly (mm mo <sup>-1</sup> )				Annual (mm yr <sup>-1</sup> )				Period-averaged (mm yr <sup>-1</sup> )		
	mv	me	de	re (%)	mv	me	de	re (%)	mv	me	re (%)
Bugac	50	-0.7	16.1	-1.4	456	-29	28.3	-6.3	-	-	-
Matra	43	1.4	14.1	3.3	401	4.4	29.2	1.1	-	-	-
Hegyhatsal	55	0.1	7.9	0.2	-	-	-	-	-	-	-
Hidegvizvolgy	-	-	-	-	-	-	-	-	620	18	2.9
Kapos	-	-	-	-	-	-	-	-	582	-56	-9.6
Marcal	-	-	-	-	-	-	-	-	559	-10	-1.8
Zagyva	-	-	-	-	-	-	-	-	531	-9	-1.7
Zala	-	-	-	-	-	-	-	-	564	11	1.9

Table 2. Error (estimated minus measured value) analysis of the ET estimates for Hungary. me: error mean; de: standard deviation of error; re: relative error (%) defined as the ratio of the error mean and the measurement mean (mv). Note that there is only one single period averaged value for each watershed, so there the mean results from one value.

A 44% underestimation by the EC technique is somewhat larger than the generally accepted 10-30% systematic undershoot (Baldochi, 2003) well known for such systems. The unusually high location and placement (82 m above ground on a 117-m TV transmitter tower) of the instruments (Barcza et al., 2009) may have contributed to the increased undershoot.

At the watershed-scale, validation is possible only in a multi-year sense because even at an annual basis water balance closure of  $P - R$  yields a highly uncertain estimate of ET due to the typically unknown changes in water storage within the catchment in the form of soil moisture and groundwater (Szilágyi & Józsa, 2009b). Period-averaged ET estimates are within a few percent of the water-balance values, except at the Kapos catchment, where CREMAP undershoots water-balance ET by about 10%. As can be seen in Fig. 2, this catchment contains the highest number of reservoirs (in fact more than is discernible from the map) having typically elongated shapes nested in the rolling terrain which are narrow enough so that they would not show up clearly in the 1-km resolution MODIS pixels as low surface temperature areas. If the (unknown) total surface area of such reservoirs is just 2% of the drainage area, then it means about a 4% increase in watershed ET due to the almost doubling of the latent heat fluxes between open water surfaces and the land (see Fig. 6). Therefore, the real undershoot in land area ET by CREMAP is probably less severe.

Fig. 8 displays the distribution of the multi-year (2000-2006) precipitation recycling index, the ratio of the mean annual ET and precipitation rates. The corresponding period is two years shorter than the study period because of the availability of water balance data for the whole country, necessary to validate the index values. When the pixel values are aggregated over the country the index becomes 0.892 versus the officially derived value of 0.896 for the same period, a remarkable match.

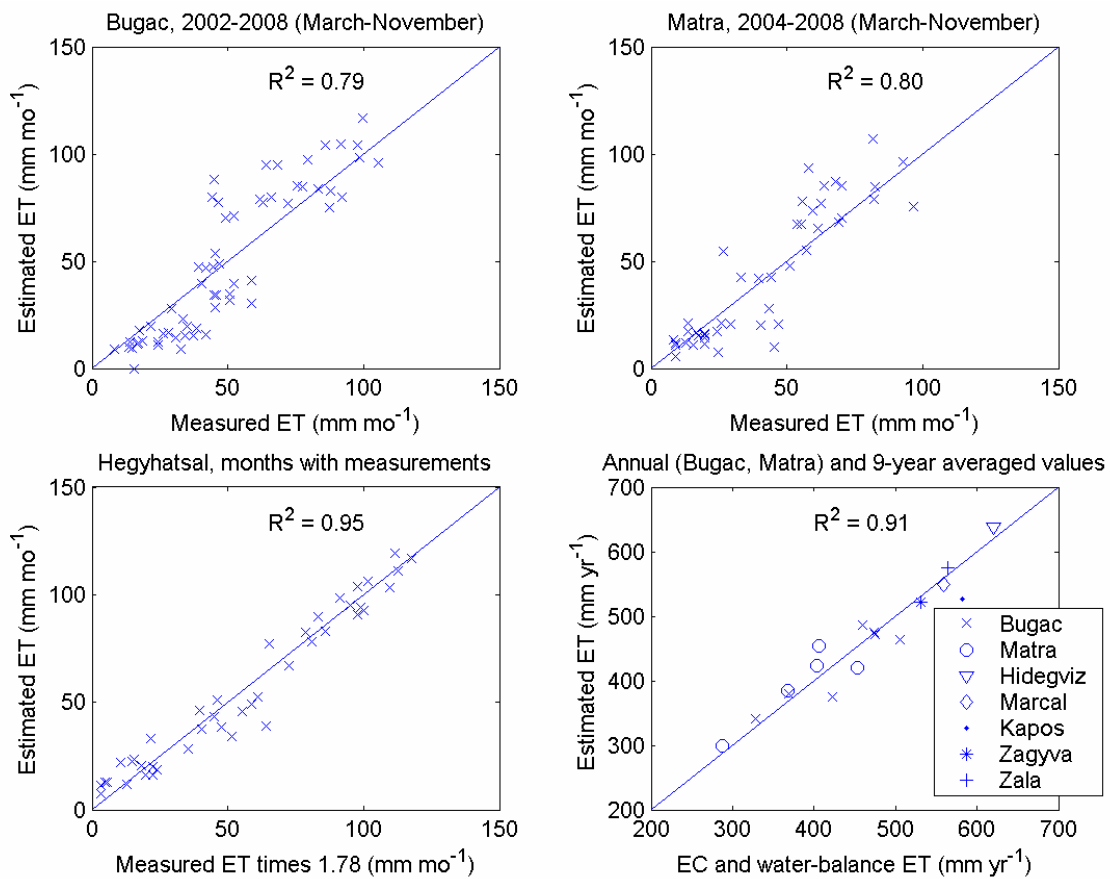


Fig. 7. Validation of the ET estimation method with eddy-covariance (Bugac, Matra and Hegyhatsal) and catchment water-balance data in Hungary.

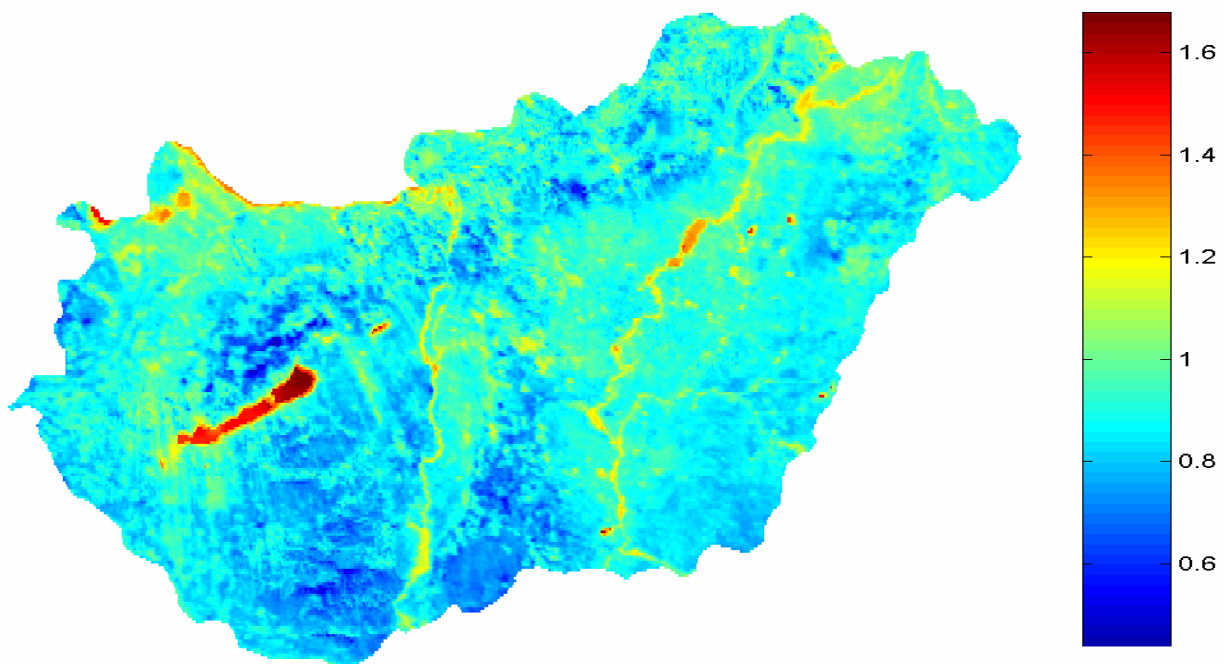


Fig. 8. Spatial distribution of the multi-year mean precipitation recycling index (ET/P) for 2000-2006 in Hungary.  $\langle ET/P \rangle = 0.89$ .

To demonstrate the practical value of the 1-km resolution ET maps in regional water resources management, let us have a look at what ET rates the maps predict for forested areas in the central inter-fluvial sand plateau region of the country, an area in focus for water resources managers due to the long-term groundwater decline (e.g., Szilágyi & Vorosmarty, 1997) reported in the region. As seen in Fig. 8, some forested areas evaporate more (the index is larger than one) than the precipitation rate they receive. This is only possible if these forests create a depression in the groundwater table, to induce local groundwater flow directed toward them which supplies the difference in ET and precipitation. In fact, this has been reported by Major (1976, in Stelczer, 2000) from the region based on piezometer measurements, where they found that under the forest the groundwater table was on average 1 m deeper than in the surrounding non-forested areas. They calculated a mean annual ET rate of 712 mm for an actively growing black spruce community covering an area of 500 x 500 m. On average the forest consumed 130 mm more water annually than it received from precipitation. Our figures match these findings, yielding an average 620 mm annual ET for the forests in the area (this value may go up to 650 mm in certain pixels), which is about 80 mm more than the mean annual precipitation rate of the region. Similar conclusion have been drawn by Szilágyi & Vorosmarty (1997) from a complex regional, coupled surface water-groundwater balance model.

#### 4.2 Nebraska, USA

The spatial distribution of the mean annual CREMAP ET values (2000-2009) in Nebraska is displayed in Fig. 9.

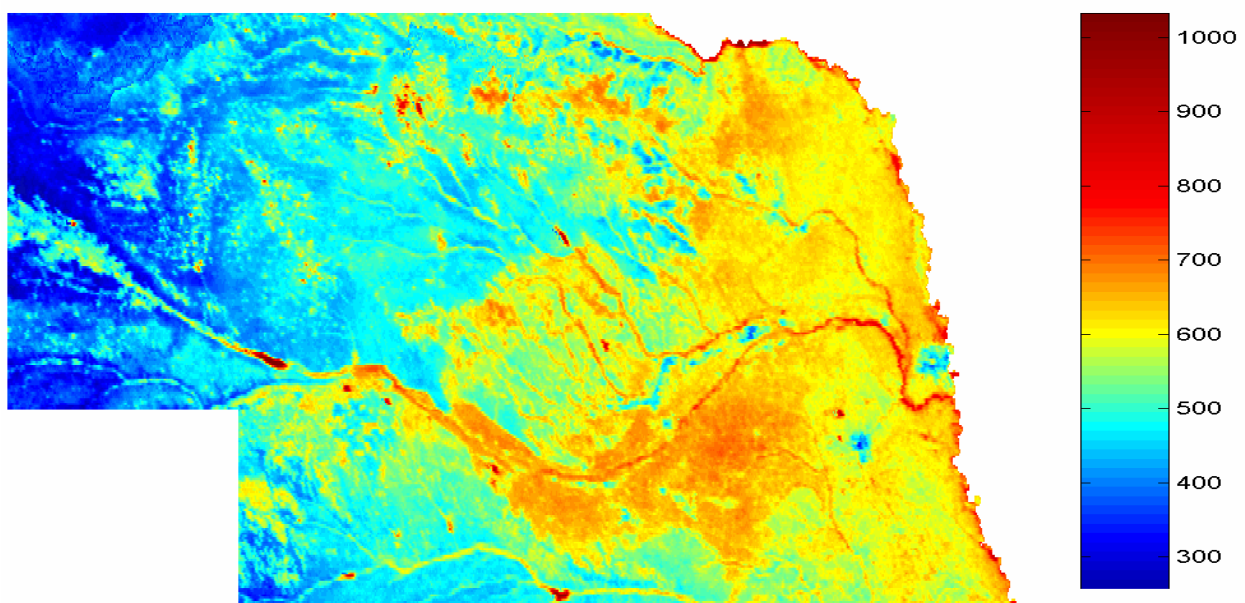


Fig. 9. Period averaged (2000-2009) mean annual ET rates (mm) in Nebraska, USA.  $\langle ET \rangle = 531 \text{ mm yr}^{-1}$ .

The high ET areas match closely the distribution of irrigation wells in the state (Fig. 10). The Sandhills region (Fig. 10) with its porous soil and grass-covered sand dunes is generally not suited for surface irrigation, thus the high ET areas within it correspond to shallow interdunal lakes prevalent mainly in the western and north-central part of the region. The river valleys with their shallow groundwater (most distinctly the Platte, flowing west to east

with its tributaries in the middle, as well as the Missouri that forms the eastern boundary of the state and the Republican River in the southern part), also show up distinctly in the ET map, such as the two largest urban areas (i.e., Omaha and Lincoln) with their reduced evaporation rates in the south-east section of the state. The largest reservoirs on the streams with their high evaporation rates are clearly visible too. Precipitation has a strong gradient across the state, exceeding 800 mm per year in the eastern part, and decreasing to nearly 300 mm per year in the western portion of it.

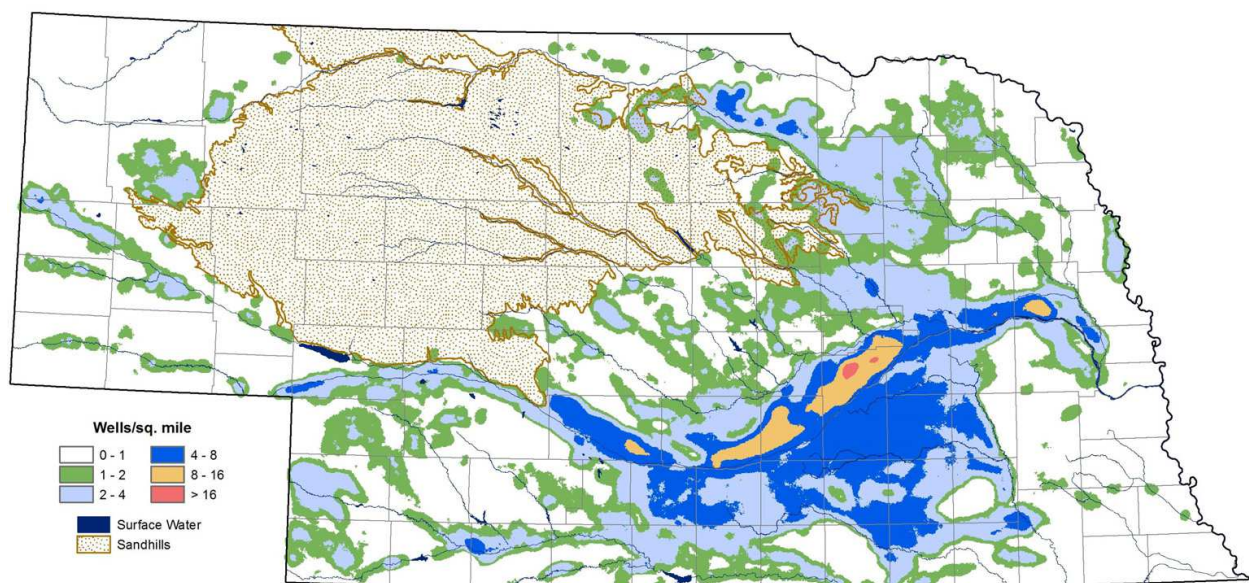


Fig. 10. Density of irrigation wells in Nebraska, 2009 (after Burbach & Korus, 2009).

The precipitation recycling index ( $ET/P$ ) is displayed in Fig. 11. Again, the stream network is clearly visible. The Sandhills region has long been known as the main recharge area of groundwater in the state due to its porous soil. As Fig. 11 indicates, recharge is highly variable even within the Sandhills, its south-eastern portion (i.e., the largest continuous dark-blue area) generating the largest amount of recharge, probably because precipitation is most abundant there within its boundaries. It is also noteworthy to mention how sharply the south-eastern boundary of the Sandhills region is distinguishable in Fig. 11, with the southernmost part reaching the Platte River, in comparison with Fig. 10. As CREMAP does not use any soil or vegetation cover information, it is remarkable that from the ET distribution of the CREMAP estimates alone it is possible to map boundaries of different physical soil types (i.e., sand vs loess). The linear dark-blue feature east of the Sandhills between the Platte and its tributary, the Loup, is also made up of sand such as the area (called the Duncan dune field) just east of it, close to the confluence.

When the index is larger than unity, it means the area has a water supply other than precipitation over the same area. For rivers and lakes the additional water supply comes from the corresponding catchment area, for irrigated land, it is the ground or surface water used for irrigation. The largest index values are found in the western part of the state where precipitation is the scarcest and for irrigated areas the relative portion of irrigated water volumes is the largest when compared to precipitation, in order to satisfy the water demand of the crop.

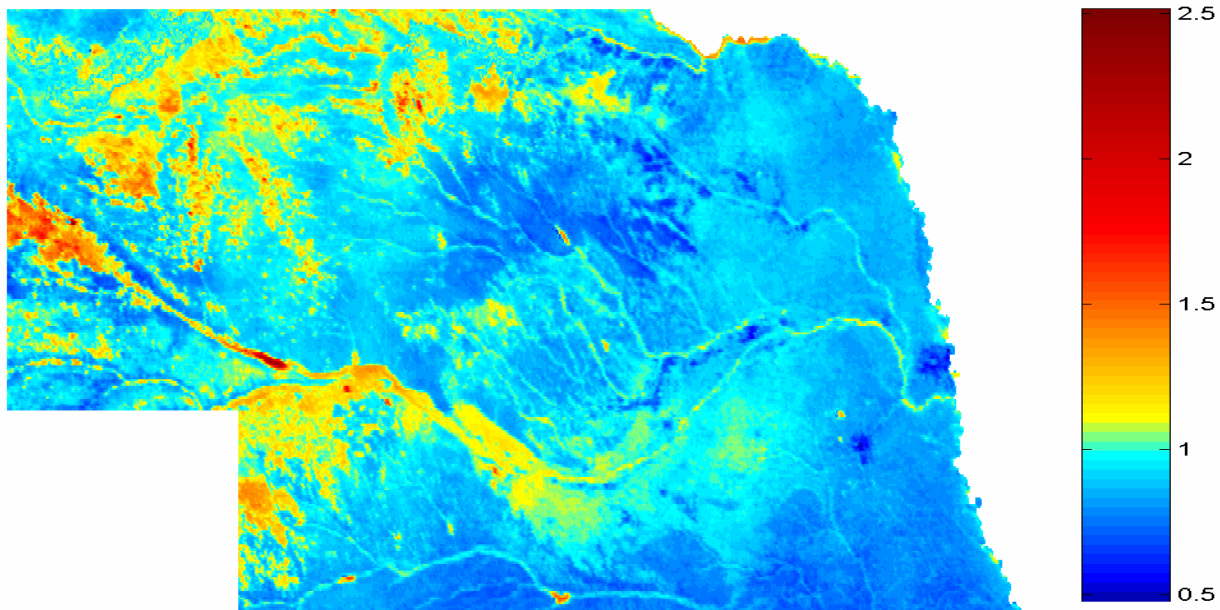


Fig. 11. The precipitation recycling index (ET/P) for 2000-2009 in Nebraska, USA.  $\langle ET/P \rangle = 0.93$ .

Table 3 displays the results of the validation at the four locations listed in Table 1.

Location	Monthly (mm mo <sup>-1</sup> )				Annual (mm yr <sup>-1</sup> )			
	mv	me	de	re (%)	mv	me	de	re (%)
Sandhills, average of 3 sites	52	5.6	17.6	10.7	471	36	55.6	7.6
Gothenburg	68	10.1	19.5	14.9	663	38	38.4	5.7
Odessa	65	7.25	19.6	11.1	623	17	50.5	2.7
Mead, average of irrig. maize & rainfed sites	69	0.6	25.5	0.8	642	-34	68.6	-5.3

Table 3. Error (estimated minus measured value) analysis of the ET estimates for Nebraska. me: error mean; de: standard deviation of error; re: relative error (%) defined as the ratio of the error mean and the measurement mean (mv).

At the Sandhills and in the Platte riparian forest, the CREMAP values tend to overestimate the measured values, probably due to differences in footprints. At both locations the MODIS pixel is larger than the footprint area of the local measurements (Table 1), thus the MODIS pixels always include wetter inter-dunal valleys in the Sandhills, and wide, open channel portions, as well as irrigated crop areas around the riparian forest locations. Because of the high spatial variance in ET over the Sandhills (ET depends heavily on whether it is a typically wet inter-dunal valley or the much drier top of a sand dune) over relatively small scales, an average of the three sites was used for comparison with MODIS-cell derived ET estimates. The difference in the resulting ET estimates (i.e., measured vs estimated) is typically stronger in the summer months (Fig. 12) when the foot-print area of the local instruments decreases due to increased buoyancy of the air (Landon et al., 2009). At the riparian forest sites the uncorrected ET-flux measurements were multiplied by 1.13 in this study in order to close the energy balance, as discussed by Landon et al. (2009). From the

two riparian sites the MODIS cell at Odessa had a better collocation with local instruments (i.e., the instrument is almost in the middle of the MODIS cell) and covered the riparian forest almost perfectly, explaining why MODIS estimates show less bias of the measured values (Table 3 and Fig. 12). At Mead, two of the plots (i.e., irrigated maize and rainfed maize/soyben) fell in one MODIS cell while the third covered only a fraction of the corresponding MODIS cell, thus the average of the two former plots were chosen for analysis.

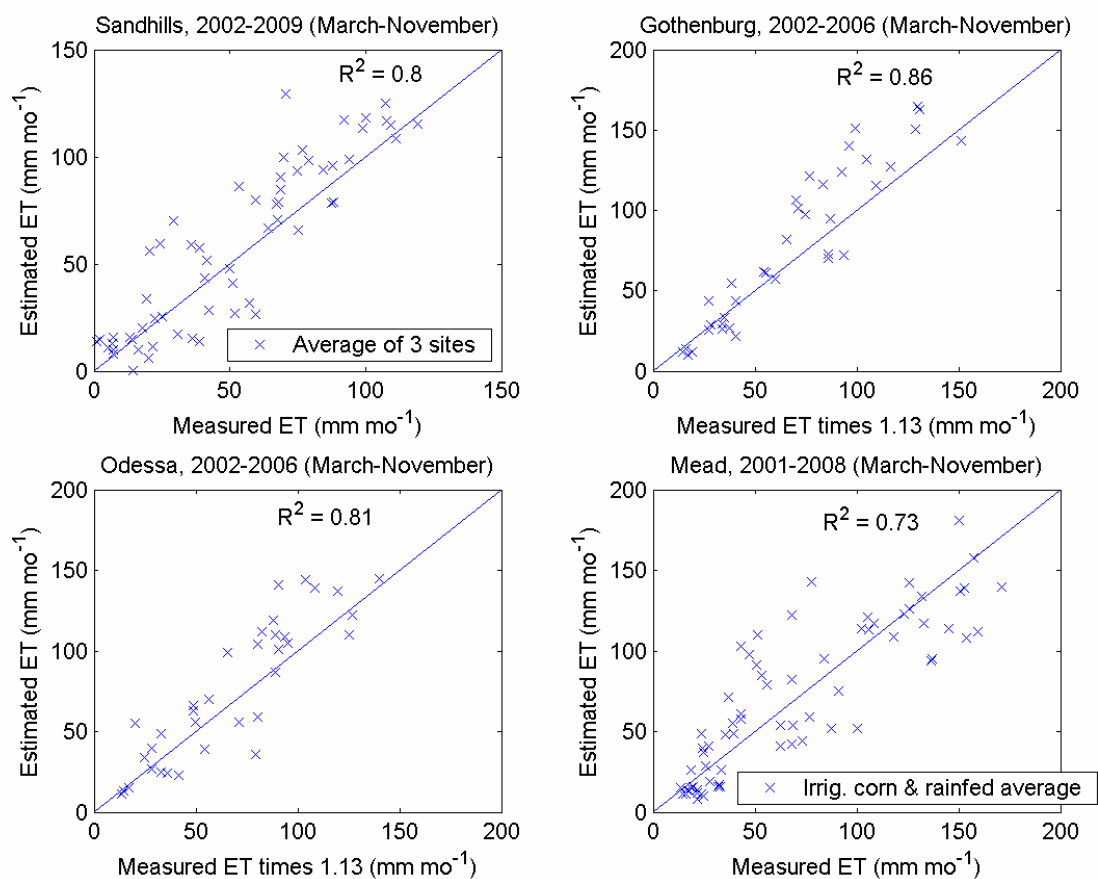


Fig. 12. Validation of the CREMAP estimates with Bowen-ratio (Sandhills and Mead) and eddy-covariance data. The EC values were multiplied by 1.13 to close the energy balance.

In Fig. 5 the smallest region in the north-western part of the country was chosen because it contains the Pine Ridge area, the most rugged part of the state. Over this area (and to a lesser degree, along the Niobrara River breaks in north-central Nebraska) the multi-year average of the CREMAP estimates is typically 15% larger than the same average of precipitation. The Pine Ridge (and the deep and wide Niobrara valley) creates increased large-scale turbulence of the air leading to a more effective heat transfer across the land/vegetation-atmosphere interface, especially that the predominant wind in the two regions is almost perpendicular to the axes of the ridge/valley. A similar problem has not been observed in Hungary because the country, due to its basin location (surrounded by the Alps and the Carpathian Mountains), is much less windy than the American prairie. Aided by an eco-region map of the state, the Pine Ridge and Niobrara River breaks could be identified in the MODIS cells, and the overlapping cell ET values corrected, so that their multi-year areal averages became constrained by precipitation.

## 5. Summary and conclusions

The present ET estimation model (CREMAP) is a modified and updated version of the ET estimation technique of Szilágyi and Józsa (2009b) and utilizes 1-km 8-day composited MODIS daytime surface temperature,  $T_s$ , and basic atmospheric data (mean air temperature and humidity as well as either sunshine duration or incident global radiation) to estimate the latent heat flux at a monthly time-step. The approach is based on a linear transformation of the mean monthly MODIS  $T_s$  pixel values into ET rates (Fig. 1). The anchor points of the transformation come from the (a) regional ET rate of the complementary relationship (Bouchet, 1963) of evaporation and the corresponding spatial mean of  $T_s$ ; (b) Priestley-Taylor equation of wet environment ET and the corresponding spatial mean of the coldest points in the region. The resulting linear equation is valid always for the given computation interval. With each month a new transformation equation is obtained similarly (Fig. 4). For typical temperate climates, such as found in Hungary, the customary value of 1.26 for  $\alpha$  is generally satisfactory in the Priestley-Taylor equation, the value of which to be reduced somewhat for drier climates (Szilágyi et al., 2009), such as the value of 1.2, applied for Nebraska. Changes in elevation can be accounted for by a linear interpolation of the parameters of the transformation equation (Eq. 5). A similar, 2-D linear interpolation can be applied for large study areas after a subdivision of them into smaller regions, as was performed for Nebraska. The advantage of the present method over that of Szilágyi and Józsa (2009b) is that the regional evaporation rate is calculated by the WREVAP model which is easier to employ than the wet-surface equation (Yeh & Brutsaert, 1971; Szilágyi & Józsa, 2009c) which needs daily maximum air temperature values, in addition of the data requirement of WREVAP, for the calculation of the daytime air temperature. The model was validated with eddy covariance (EC) and Bowen-ratio (BR) station measurements plus catchment-scale water-balance closure data. The validation, spanning almost three magnitudes in spatial scale (Table 1), indicated a favorable match between ET estimates and observations (Figs. 7 & 12; Tables 2 & 3). On a monthly basis the ET estimates resulted in an  $R^2$  value of 0.8 – 0.9 with a minimum value of 0.73 and maximum of 0.95. During validation a problem arises from differences in foot-print areas between local measurements and the MODIS cell. As a consequence, more weight is to be given to validation results where the two foot-print sizes match, such as a) at Hegyhatsal ( $R^2 = 0.95$ ) where the strong linear correspondence with measurements and high accuracy of the ET estimates result from high-tower mounted (82 m above ground) EC instruments, and; b) at the watersheds in Hungary, which thus yield improved statistics. At the rest of the EC and BR validation sites the instruments sample a smaller area than the size of the MODIS pixel. The overall strong correspondence with measured ET values and unbiased nature of the ET estimates are generally maintained at the annual and multi-annual level (Fig. 9; Tables 2 & 3), where seasonality effects are eliminated. On an annual and multi-year basis a typical value of  $R^2$  is between 0.7 – 0.8 with a minimum of 0 (this happened at the riparian forest sites where inter-annual variance of ET is much reduced) and maximum of 0.91. The mean annual ET estimates remain well within 10% of the measured values.

The model is simple, requires only a minimum amount of easily accessible data, and calibration free. From the first author's personal website documentation of the WREVAP program with its FORTRAN source code is also accessible. The WREVAP program can be applied separately to estimate evaporation from open water surfaces. Typically mean annual open water evaporation is in excess of the CREMAP estimate by about 10%, mainly due to differences in albedo between the land and water.

Generally, CREMAP is expected to work correctly in areas where the CR is valid (Szilágyi et al., 2009). In its present form, it is not recommended to be applied in mountainous areas or in areas with strong surface-albedo and/or momentum roughness height changes at a scale in excess of 1-km. Also, due to its inherent assumptions (i.e., a spatially constant  $Q_n$  and aerodynamic resistance as well as the application of the Priestley-Taylor equation), it is not recommended to be applied at a spatial resolution finer than 1-km.

Research is currently undertaken to extend the method to conditions when the spatially constant  $Q_n$  requirement is violated. Employing high-resolution digital elevation models and MODIS surface albedo data, known changes in albedo, mean surface slope and aspect among the MODIS cells can be accounted for in the transformation equations. Further research is required to investigate the aerodynamic resistance altering effect of rolling-to-rugged terrain transitions and the inclusion of such effects in the modeling framework.

## 6. Acknowledgments

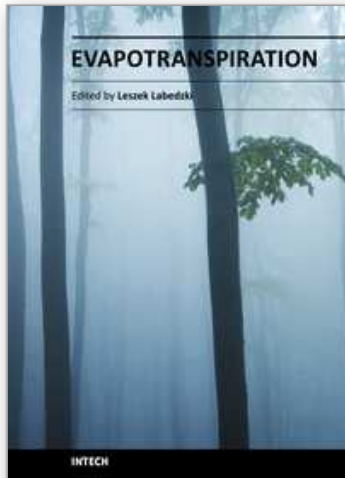
This work has been supported by the Hungarian Scientific Research Fund, #77364. We thank G. Antal, Z. Barcza, D. Billesbach, A. Clement, Z. Gribovszki, L. Haszpra, P. Kalicz, L. Sütő, J. Szalai, USGS-Lincoln, G. Varga, & S. Verma for their data.

The views, conclusions, and opinions expressed in this study are solely those of the writers and not the University of Nebraska, state of Nebraska, or any political subdivision thereof.

## 7. References

- Allen, R.; Tasumi, M. & Trezza, R. (2007). Satellite-based energy balance for mapping evapotranspiration with internalized calibration (METRIC)-model. *J. Irrig. Drainage Eng.*, 133(4), 380-394.
- Baldocchi, D. (2003). Assessing the eddy covariance technique for evaluating carbon dioxide exchange rates of ecosystems: past, present and future. *Global Change Biol.*, 9, 1-14.
- Barcza, Z.; Kern, A.; Haszpra, L. & Kljun, N. (2009). Spatial representativeness of tall tower eddy covariance measurements using remote sensing and footprint analysis. *Agric. Forest Meteorol.*, 149, 795-807.
- Bastiaanssen, W.; Menenti, M.; Feddes, R. & Holtslag, A. (1998). A remote sensing surface energy balance algorithm for land (SEBAL): 1. Formulation. *J. Hydrol.*, 212, 198-212.
- Bouchet, R. (1963). Evapotranspiration réelle, evapotranspiration potentielle, et production agricole. *Annal. Agronom.*, 14, 543-824.
- Brutsaert, W. & Parlange, M. (1998). Hydrologic cycle explains the evaporation paradox. *Nature*, 396(6706), 30.
- Brutsaert, W. & Stricker, H. (1979). An Advection-Aridity approach to estimate actual regional evapotranspiration. *Water Resour. Res.*, 15, 443-449.
- Burbach, M. & Korus, J. (2009). Density of active irrigation wells in Nebraska. Conservation & Survey Division, Institute of Agricultural and Natural Resources, University of Nebraska - Lincoln, <http://snr.unl.edu/data/water/groundwatermaps.asp>
- Hobbins, M.; Ramirez, J. & Brown, T. (2001a). The complementary relationship in estimation of regional evapotranspiration: An enhanced advection-aridity model. *Water Resour. Res.*, 37(5), 1389-1403.
- Hobbins, M.; Ramirez, J.; Brown, T. & Claessens L. (2001b). The complementary relationship in estimation of regional evapotranspiration: The complementary relationship areal evaporation and advection-aridity models. *Water Resour. Res.*, 37(5), 1367-1387.

- Landon, M.; Rus, D.; Dietsch, B.; Johnson, M. & Eggemeyer, K. (2009). Evapotranspiration rates of riparian forests, Platte River, Nebraska, 2002-06. *USGS Report 2008-5228*.
- Major, P. (1976). Groundwater balance investigations in flat lands. 2. Piezometer readings. (VITUKI report, in Hungarian), VITUKI, Budapest.
- Morton, F.; Ricard, F. & Fogarasi, S. (1985). Operational estimates of areal evapotranspiration and lake evaporation - Program WREVAP. National Hydrological Research Institute Paper #24, Ottawa, Ontario, Canada.
- Nagy, Z.; Pintér, K.; Czóbel, S.; Balogh, J.; Horváth, L.; Fóti, S.; Barcza, Z.; Weidinger, T.; Csintalan, Z.; Dinh, N.; Grósz, B. & Tuba, Z. (2007). The carbon budget of semi-arid grassland in a wet and a dry year in Hungary. *Agric. Ecosyst. Environ.*, 121, 21-29.
- Penman, H. (1948). Natural evaporation from open water, bare soil, and grass. *Proc. Royal Soc. London*, A193, 120-146.
- Pintér, K.; Barcza, Z.; Balogh, J.; Czóbel, S.; Csintalan, Z.; Tuba, Z. & Nagy, Z. (2008). Interannual variability of grasslands' carbon balance depends on soil type. *Community Ecol.*, 9(Suppl1), 43-48. doi: 10.1556/ComEc.9.2008.S.7.
- Priestley, C. & Taylor, R. (1972). On the assessment of surface heat flux and evaporation using large-scale parameters. *Month. Weather Rev.*, 100, 81-92.
- Stelczer, K. (2000). A vízkészletgazdálkodás hidrológiai alapjai (Hydrological bases of water resources management, in Hungarian). ELTE Eotvos Kiado, Budapest, Hungary.
- Szilágyi, J. (2001). Modeled areal evaporation trends over the conterminous United States. *J. Irrig. Drainage Engin.*, 127(4), 196-200.
- Szilágyi, J. & Vorosmarty, C. (1997). Water-balance modeling in a changing environment: reductions in unconfined aquifer levels in the area between the Danube and Tisza rivers in Hungary. *J. Hydrol. Hydromech.*, 45, 348-364.
- Szilágyi, J. & Józsa, J. (2008). New findings about the complementary relationship based evaporation estimation methods. *J. Hydrol.*, 354, 171-186.
- Szilágyi, J.; Hobbins, M. & Józsa, J. (2009). A modified Advection-Aridity model of evapotranspiration. *J. Hydrol. Engin.*, 14(6), 569-574.
- Szilágyi, J. & Józsa, J. (2009a). Analytical solution of the coupled 2-D turbulent heat and vapor transport equations and the complementary relationship of evaporation. *J. Hydrol.*, 372, 61-67.
- Szilágyi, J. & Józsa, J. (2009b). Estimating spatially distributed monthly evapotranspiration rates by linear transformations of MODIS daytime land surface temperature data. *Hydrol. Earth System Sci.*, 13(5), 629-637.
- Szilágyi, J. & Józsa, J. (2009c). An evaporation estimation method based on the coupled 2-D turbulent heat and vapor transport equations. *J. Geophys. Res.*, 114, D06101. doi:10.1029/2008JD010772.
- Yeh, G. & Brutsaert, W. (1971). A solution for simultaneous turbulent heat and vapor transfer between a water surface and the atmosphere. *Bound. Layer Meteorol.*, 2, 64-82.



## **Evapotranspiration**

Edited by Prof. Leszek Labeledzki

ISBN 978-953-307-251-7

Hard cover, 446 pages

**Publisher** InTech

**Published online** 16, March, 2011

**Published in print edition** March, 2011

Evapotranspiration is a very complex phenomenon, comprising different aspects and processes (hydrological, meteorological, physiological, soil, plant and others). Farmers, agriculture advisers, extension services, hydrologists, agrometeorologists, water management specialists and many others are facing the problem of evapotranspiration. This book is dedicated to further understanding of the evapotranspiration problems, presenting a broad body of experience, by reporting different views of the authors and the results of their studies. It covers aspects from understandings and concepts of evapotranspiration, through methodology of calculating and measuring, to applications in different fields, in which evapotranspiration is an important factor. The book will be of benefit to scientists, engineers and managers involved in problems related to meteorology, climatology, hydrology, geography, agronomy and agricultural water management. We hope they will find useful material in this collection of papers.

### **How to reference**

In order to correctly reference this scholarly work, feel free to copy and paste the following:

József Szilágyi, János Józsa and Ákos Kovács (2011). A Calibration-Free Evapotranspiration Mapping (CREMAP) Technique, Evapotranspiration, Prof. Leszek Labeledzki (Ed.), ISBN: 978-953-307-251-7, InTech, Available from: <http://www.intechopen.com/books/evapotranspiration/a-calibration-free-evapotranspiration-mapping-cremap-technique>

**INTECH**  
open science | open minds

### **InTech Europe**

University Campus STeP Ri  
Slavka Krautzeka 83/A  
51000 Rijeka, Croatia  
Phone: +385 (51) 770 447  
Fax: +385 (51) 686 166  
[www.intechopen.com](http://www.intechopen.com)

### **InTech China**

Unit 405, Office Block, Hotel Equatorial Shanghai  
No.65, Yan An Road (West), Shanghai, 200040, China  
中国上海市延安西路65号上海国际贵都大饭店办公楼405单元  
Phone: +86-21-62489820  
Fax: +86-21-62489821

© 2011 The Author(s). Licensee IntechOpen. This chapter is distributed under the terms of the [Creative Commons Attribution-NonCommercial-ShareAlike-3.0 License](#), which permits use, distribution and reproduction for non-commercial purposes, provided the original is properly cited and derivative works building on this content are distributed under the same license.

IntechOpen

IntechOpen